Experimental Assessment of the Depth of the Deformed Layer in the Roller Burnishing Process

Marek Kowalik[1,*], and *Tomasz* Trzepiecinski[1]

[1]Kazimierz Pulaski University of Technology and Humanities in Radom, Institute of Mechanical Engineering, ul. Krasickiego 54, 26-600 Radom, Poland
[2]Rzeszow University of Technology, Department of Materials Forming and Processing, al. Powst. Warszawy 12, 35-959 Rzeszów, Poland

Abstract. This paper presents the methods of experimental determining the depth of the plastically deformed top layer in the roller burnishing process. Precise determination of the depth of the plastically deformed layer is difficult due to slight deformation at the boundary of the plastic and elastic zone, the lack of visible changes in the microstructure, and minimal changes in microhardness. The article shows the method of original measurement method that consists in determining the thickness of the deformed layer using rings. The method involves the profilographometric measurements of the disconnected rings (samples) which are flat-faced in the package on the mandrel. The rings material deforms plastically in the surface layer causing wrapping of the end face of the ring in the direction of the rolling tool movement. After dismantling the ring pack, measurements were made on the face of each ring along radial directions, and the thickness of the deformed layer was observed on the microscope. The method was verified by microhardness measurements in the cross-section and cross-section of the ring. The results of deformation depth measurements were verified by finite-element-based numerical simulation.

1 Introduction

The roller burnishing (RB) process is used when the goal is to achieve a high-quality surface finish strengthened by the strain hardening phenomenon [1-2]. Many material forming technologies such as burnishing, thread rolling, spline rolling, knurling, drawing lead to both the deformation of the surface layer of the material and changes of its properties. This phenomenon of cold plastic deformation introduces the compressive stresses into the surface layer increasing its surface hardness, and both static and fatigue strength [1, 2]. Under the pressure of rounded tool the small layer deformation occurs not only in plastic forming processes but also in turning, milling, grinding [3] or even laser surface treatment [4-6]. The scale of plastic deformation in the above-mentioned processes

* Corresponding author: m.kowalik@uthrad.pl

is smaller than in roller burnishing, but it is always possible to observe a plastically deformable surface layer. Plastic deformations of metal surface can occur under relatively small forces, i.e. even during measurements or assembly [7-9]. Roller burnishing causes the strain hardening of the material and introduces compressive stresses into surface layer that increase the hardness [10], the strength of the surface layer of the material [11]. In the case of machine parts exposed to fatigue, the depth of the deformed layer becomes the basic factor determining the technological parameters of rolling [4]. The main purpose of the strengthened burnishing process is to obtain the maximum possible depth of plastic deformation in the surface layer [11-12] which will not cause microcracking of the surface of workpiece [13].

Roller and ball burnishing have been studied by a number of researchers on various materials. El-Axir [14] found that the burnishing feed and burnishing force feed have the most significant effect on both microhardness and surface roughness. Luo et al. [15] studied the effect of the burnishing parameters on the burnishing force and material microhardness via theoretical analysis. The results showed that burnishing depth and feed were the most significant factors. Franzen et al. [16] found that the rolling process parameters had a great influence on the tribological properties of burnished surfaces. Balland et al. [17] propose finite element 3D modelling of the ball burnishing process and analysed the effect of the burnishing parameters on the properties of the surface material. They concluded that the mechanism of formation and flow of the ridge appears to have a central role in the treatment of a surface by burnishing. The effects of the initial surface roughness and hardness of the workpiece, the lubricant, and the burnishing tool geometry on material hardness were studied by Hassan and Maqableh [18] and Loh et al. [19]. Hamadache et al. [20] developed a device for mechanical plastic deformation of structural steel using roller burnishing and for investigating the evolution of surface roughness, hardness and wear resistance. The optimum hardness and roughness were obtained for a specific regime whose decisive parameters are the applied force and the number of passes of the burnishing tool. El-Tayeb et al. [21] investigated the influence of the contact conditions between the roller and workpiece on the quality of the burnished surface as well as tribological behaviour in roller burnishing.

Kowalik et al. [22] and Kowalik and Trzepiecinski [23] showed that the depth of the plastically deformed layer in the burnishing process is influenced by the state of stress during roller burnishing process. The asymmetric state of stress caused by the roll braking during burnishing [23] causes a greater depth of plasticised zone in the surface layer of shaft. Almost all researchers in the works cited above, the depth of plastic deformation of the surface layer identify with the area with increased hardness of the material as a result of plastic deformation. This is an imprecise opinion because a noticeable increase in hardness of the material is possible only under the influence of significant plastic deformations [9]. Agrawal and Singh obtained a 5% hardness increase of steel samples at the amount of plastic deformation of 60% and small changes in the metallographic structure [24]. Wang et al. [25] and Fazil et al. [26] found small changes in hardness as a function of deformation despite a significant increase in the material strength.

This paper presents the method for determining the depth of plastic deformation of the surface layer in the process of roller burnishing. The depth of the deposition of plastisised layer is determined on the basis of hardness measurement in the specimen cross-section, observation of the metallographic structure and measurement of deformation of the ring faces after the roller burnishing process. Experimentally determined depths of the plasticised surface layer were verified based on the results of finite element (FE) modeling.

2 Experimental

Experimental tests were carried out on ring-shaped samples (Fig. 1a). The samples were matched into a stack on the pin. The top layer of the material of the rings is deformed plastically, causing curling of the end face of the rings in the direction of movement of the roller. A significant deformation was observed on the end faces of the rings, which does not cause their separation (the faces of the rings are in permanent contact). Three measuring rings with an outer diameter of d = 75 mm and a thickness of 15 mm (2-4 in Fig. 1a) are fastened between two supporting discs (1 and 5 in Fig. 1a) with a thickness of 20 mm. The working diameter of the pin was equal to d_p = 30 mm. The samples were burnished at different values of roller force and different values of braking moment. The depth of plastic deformation in the surface layer was measured on the faces of the samples. After dismounting the set of rings, measurements were carried out on the faces of each ring along the radial running lines and the thickness of the plastically deformed layer δ was determined (Fig. 1b).

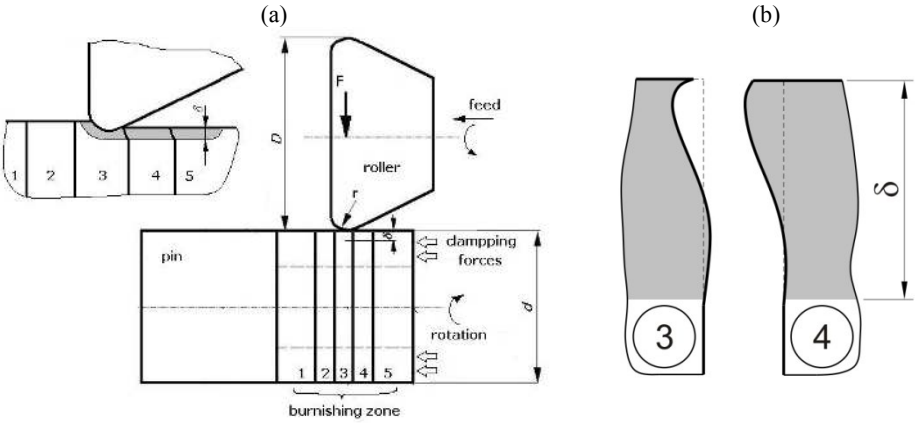

Fig. 1. A method for measuring the depth of plastic deformation of the top layer by using rings: (a) schematic diagram of the method, (b) magnification of the top layer of neighbouring rings no. 4 and 5 after dismounting.

3 Numerical modeling

A numerical simulation of the roller burnishing is carried out using the FE-package MSC.Marc + Mentat. The geometry of the FE-based model is corresponded to the experimental geometry (Fig. 1). Both the forming roller and the mandrel were considered to be rigid. The longitudinal movement of the roller and rotational speed of the workpiece corresponded to real conditions. The thrust force applied to the roller was 3 kN.

The mechanical properties of the ring material (heat-treatable carbon steel C45) were determined in a uniaxial tensile test, and the hardness was determined by the Rockwell method. These properties are as follows: yield stress 402 MPa, ultimate tensile stress 658 MPa, elongation 17% and hardness 231 HB. The work hardening phenomenon is described by Hollomon equation which is a power law relationship between the stress and the amount of plastic strain:

$$\sigma = K \cdot \varepsilon^n \tag{1}$$

where: K is the strength coefficient, n is the strengthening exponent.

The values of parameters in Hollomon equation are as follows: strength coefficient 1032 MPa, strengthening exponent $n = 0.134$. The elastic material parameters assumed in calculations for C45 steel are Young's modulus $E = 2.1 \cdot 10^5$ GPa and Poisson's ratio $\nu = 0.3$. The model of the pin and rings consisted of 63360 8-node isoparametric brick elements. The mesh density is the main parameter influencing the computational accuracy of the results, especially in the case of small deformations of material. Therefore the outer layer of the shaft, in which the greatest strains appeared, was divided more densely in order to improve the accuracy of the results.

4 Results and discussion

Fig. 2 shows the rings made of C45 steel after burnishing with the roller pressure F = 3 kN. The trial was carried out on a pack of three measuring rings, which were clamped on the mandrel with stopper rings 1 and 5 (Fig. 1a). This burnishing trial was carried out without a braking moment. Next the rings were disassembled and their faces (Fig. 2) were measured in the area of the deformation zone using an optical microscope, the depth of the deformed layer was equal to $\delta = 1.2$ mm. Visible tracks (Fig. 2a) on the face of the rings in the form of a series of parallel scratches are a result of the grinding process. The plastic deformation in the surface layer does not change the texture of the ground surface.

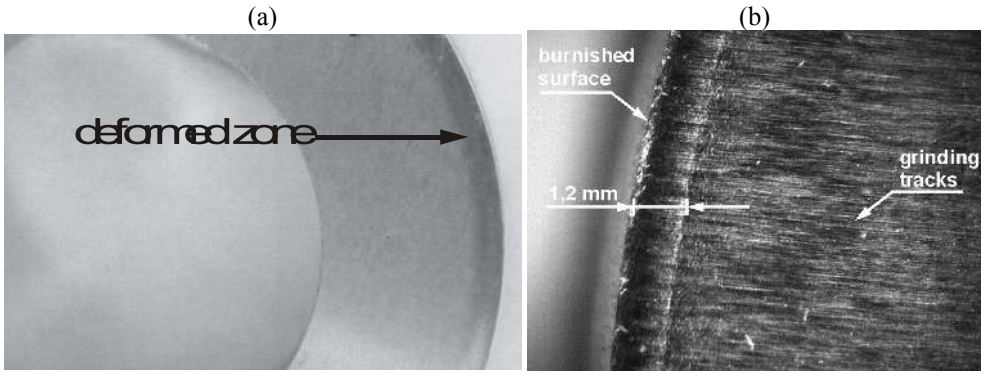

Fig. 2. View of the ring after dismantling: (a) face of the ring with a deformed layer, (b) photograph of face of rings no. 3 after burnishing with a pressure force F = 3 kN, deformed zone 1.2 mm.

In order to determine the depth of plasticised layer, the examinations of metallographic specimens were carried out. The samples for making metalographic specimens were taken from the burnished rings in cross-section and longitudinal section. Next they were polished and etched to allow observation of the microstructure on a metallographic microscope. The microstructure of the C45 steel ring in the undeformed zone consists of dark perlite grains separated by white ferrite precipitates. Fig. 3 shows the microstructure of the ring in the area of deformation at 200× magnification. A deformed layer reaching about 0.7 mm deep into the material was identified. The surface layer of plastically deformed material can be characterized by two characteristic zones. The surface layer consists of intensely deformed perlite grains and finely divided ferrite grains. The depth of this zone is about 0.3 mm, it is clearly separated from the subsurface zone. In figure 3. the depth of the subsurface zone is marked. The transition border to the subsurface zone is very clear and easy to determine.
It is more difficult to determine the transition zone between the undeformed material and the plastically deformed layer. Furthermore, it is difficult to identify very small plastic deformations on the metallographic specimens. As a boundary of the transition of undeformed material into the deformed zone the area in which one can observe the change

of the character of the ferrite network is assumed. In the undeformed zone, the ferrite network is clearer, the grains have a wider width and numerous branches and beads. In the zone of plastic deformation, the ferrite grains have a smaller thickness, the branches and beads disappear.

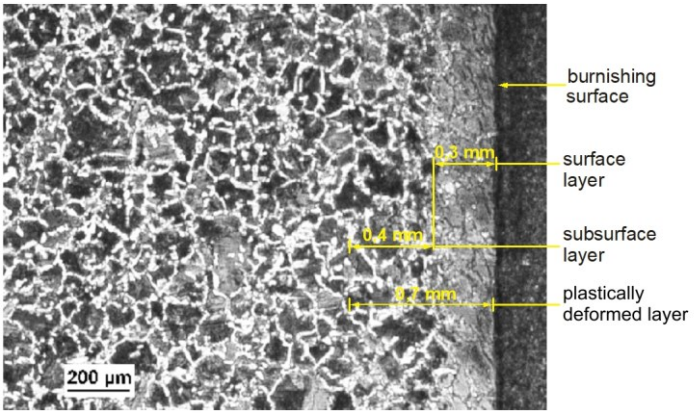

Fig. 3. Microstructure of the plastically deformed surface layer. Magnification 200x.

HV hardness measurements were made on the transverse and longitudinal sections of specimens. The indenter load was selected so that the impression during the test included several grains, because the ferrite and pearlite grains had significantly different hardnesses, the danger of measuring the hardness of individual grains was avoided. In this way, the average nature of hardness measurement was obtained. The hardness measurement was made from the surface layer into the material with a step of 0.05 mm. The first hardness measurement was made at a distance of 0.05 mm from the surface. Fig. 4 shows the hardness characteristics of the surface layer of burnished ring. In the surface layer in the depth range up to approximately of 0.3 mm clear changes in hardness are observed. It corresponds to microstructural changes observed on metallographic specimens (Fig. 3). In the deeper layers of the material, the changes in hardness are small, despite the fact that the changes in the microstructure are observed. The depth values of the plasticised layer obtained from surface hardness measurements and observations of the metallographic microstructure are much smaller than those recorded on the faces of the rings.

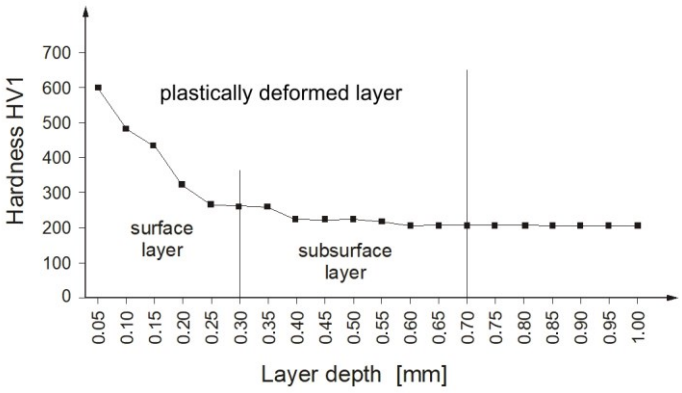

Fig. 4. Effect of the distance from the surface layer on the value of hardness HV1 in the ring cross-section.

The distribution of the equivalent plastic strain in the plasticised layer of the material is presented in Fig. 5. In order to clearly display the results, the distribution has been limited to the quarter of the model. The comparison of the numerically predicted plastised depth of the surface layer with experimental measurements is very difficult. The experimental detection of the very small values of plastic deformations is limited to the lack of the visible transition zone between undeformed and deformed material in the photograph of the face of the rig (Fig. 3b). The transition zone between elastic and plastic zone is very diffused. So, the numerically predicted value of the depth of plasticised zone (2.731 mm – Fig. 6) is higher compared to the experimental measurements.

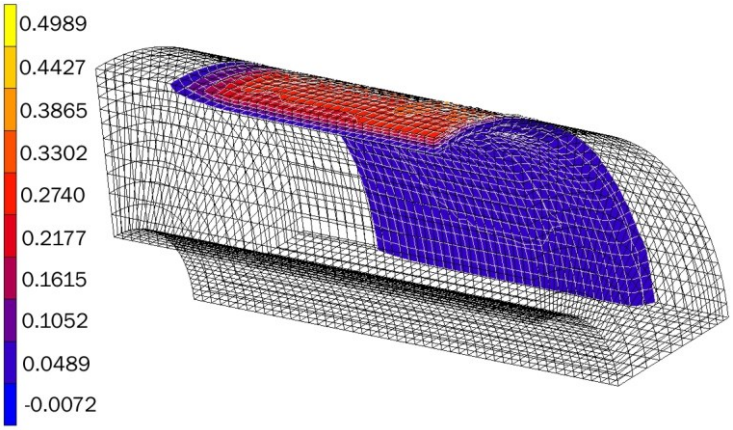

Fig. 5. The distribution of the equivalent plastic strain in plasticised zone.

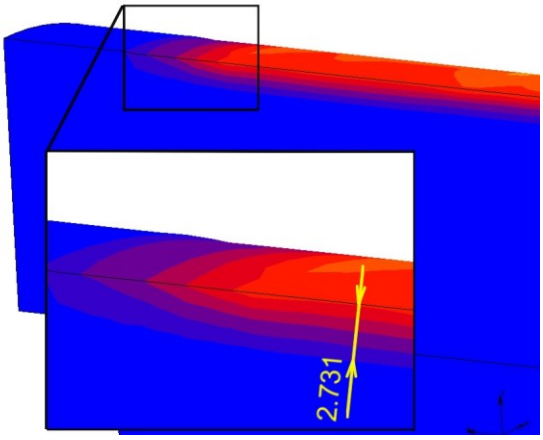

Fig. 6. The depth of the plasticized zone after roller burnishing with a force of 3 kN.

5 Conclusions

The depth of the plasticised layer in the burnishing process determined by the method of measuring the hardness and observation of the metallographic structure is very similar. The plastically deformed surface layer can be divided into two characteristic zones. A surface layer is characterized by a large deformation of the grains of the metallographic structure and a large increase in hardness. The subsurface area is clearly separated from the surface layer and is characterized by less visible deformations of the microstructure with a small

increase in hardness in relation to the undeformed material. Two-fold greater depth of plastically deformed layer was obtained by observing the faces of the rings in FE-based numerical simulation. Thus, through the widely used method of hardness measurement, only the deformations of material with very high amount can be found, and the small deformations cannot be identified.

References

1. A. Kułakowska, L. Kukielka, K. Kukielka, R. Patyk, L. Malag, L. Bohdal, Appl. Mech. Mater. **474**, 442–447 (2014)
2. L. Malag, L. Kukielka, K. Kukielka, A. Kułakowska, L. Bohdal, R. Patyk, Appl. Mech. Mater. **474**, 454–459 (2014)
3. G. Totten, M. Hower, T. Inove, *Handbook of residual stress and deformation of steel* (ASM International, Materials Park, 2002).
4. P. Zhang, J. Lindemann, W. J. Ding, C. Leyens, Mater. Chem. Phys., **124**, 835–840 (2010)
5. J. Jaworski, T. Trzepieciński, Kovove Materialy-Metallic Materials, **54**, 17–25 (2016)
6. W. Napadłek, Mater. Testing, **57**, 920–924 (2015)
7. M. Kowalik, M. Rucki, P. Paszta, R. Gołebski, Meas. Sci. Rev. **16**, 1–6 (2016)
8. M. Okada, S. Suenobu, K. Watanabe, Y. Yamashita, N. Asakawa, Mechatronics **29**, 110–118 (2015)
9. M. Kowalik, Mater. Sci., **46**, 679–684 (2011)
10. M. Kowalik, Arch. Civ. Mech. Eng. **10**, 45–56 (2010)
11. B. Zabkar and J. Kopač, J. Prod. Eng., **16**, 45–48 (2013)
12. B. P. Rusyn, N. P. Anufrieva, N. R. Hrabov'ska, V. H. Ivanyuk, Mater. Sci., **49**, 516–524 (2014)
13. B. P. Rusyn, R.V. Torska, M. I. Kobasyar, Application of the cellular automata for obtaining pitting images during simulation process of their growth, in *Man-Machine Interactions* 3, Advances in Intelligent Systems and Computing 242, edited by A. Gruca et al. (Springer, Cham, 2014), pp. 299–306
14. H. El-Axir, Int. J. Mach. Tools Manuf. **40**, 1603–1617 (2000)
15. H. Luo, J. Liu, L. Wang, Q. Wang, Int. J. Adv. Manuf. Technol. **28**, 707–713 (2006)
16. V. Franzen, M. Trompeter, A. Brosius, A. E. Tekkaya, Int. J. Mater. Form. **3**, 147–150 (2010)
17. P. Balland, L. Tabourot, F. Degre, V. Moreau, Precis. Eng. **37**, 129–134 (2013)
18. A. M. Hassan, A. M. Maqableh, J. Mater. Proc. Technol. **102**, 115–121 (2000)
19. N. H. Loh, S. C. Tam, S. Miyazawa, Prec. Eng. **15**, 100–105 (1993)
20. H. Hamadache, L. Laouar, N. E. Zeghib, K. Chaoui, J. Mater. Process. Technol. **180**, 130–136 (2006)
21. N. S. M. El-Tayeb, K. O. Low, P. V. Brevern, J. Mater. Process. Technol. **186**, 272–278 (2007)
22. M. Kowalik, T. Mazur, T. Trzepieciński, Strength Mater. **50**, 493–503 (2018).
23. M. Kowalik, T. Trzepieciński, AIP Conf. Proc. **1960,** 040011 (2018)
24. A. K. Agrawal, A. Singh, Mater. Sci. Eng. A **687**, 306–312 (2017)
25. H. T. Wang, N. R. Tao, K. Lu, Scripta Mater. **68** 22–27 (2013)
26. F. O. Sonmez, A. Demir, J. Mater. Process. Technol. **186,** 163–173 (2007)